NOTES AND CORRESPONDENCE

Shear Parameter Thresholds for Forecasting Tornadic Thunderstorms in Northern and Central California

JOHN P. MONTEVERDI

San Francisco State University, San Francisco, California

CHARLES A. DOSWELL III*

National Severe Storms Laboratory, Norman, Oklahoma

GARY S. LIPARI

San Francisco State University, San Francisco, California

14 March 2001 and 20 June 2002

ABSTRACT

A study of 39 nontornadic and 30 tornadic thunderstorms (composing 25 tornado ''events,'' as defined in the text) that occurred in northern and central California during the period 1990–94 shows that stratification of the stronger tornadic events (associated with F1 or greater tornadoes) on the basis of 0–1- and 0–6-km positive and bulk shear magnitudes is justified statistically. Shear values for the weaker F0 events could not be distinguished statistically from the ''background'' values calculated for the nontornadic (null) thunderstorm events observed during the period. Shear magnitudes calculated for the F1/F2 events suggest that these tornadoes had developed in an environment supportive of supercell convection. Hindcasting the tornado events based upon shear thresholds produced a high probability of detection (POD) and low false alarm ratio (FAR), particularly for the stronger (F1/F2) events. Although the current sample size is limited and the conclusions drawn from it should be considered preliminary, it appears that California forecasters may be able to use shear profiles to distinguish days on which there is a higher threat of storms producing moderate and significant tornadoes. Buoyancy, as indicated by surface-based convective available potential energy (SBCAPE), was weak for each of the categories, and there were no statistically significant differences between SBCAPE values for each of the categories. Thus, as is true elsewhere, buoyancy magnitude *alone* appears to be of no value in forecasting whether California thunderstorms will be tornadic.

1. Introduction

California tornadic thunderstorms[1] and their counterparts in other parts of the world in similar climatological environments (e.g., Hanstrum et al. 1998) have only recently been subjected to systematic documentation. Indeed, preconceived notions persist that tornadic storms either are not a forecasting problem in California or are ''freak'' events (see Monteverdi and Quadros 1994).

Although the processes that interact to produce tornadic storms in California are not unique, topographic effects in the Central Valley and the coastal valleys act to increase the magnitude of the vertical wind shear locally. This has been noted in previous studies, but only for a limited number of cases (e.g., Monteverdi and Quadros 1994).

In order to document the shear and buoyancy environment in this portion of the state more systematically, the detailed analysis of 30 tornadic thunderstorm cases in northern and central California during the period 1990–94 presented in Lipari and Monteverdi (2000, hereafter referred to as LM) was augmented with a study of the 41 *nontornadic* thunderstorm cases (hereinafter referred to as ''null'' cases) that occurred during the same

[1] All of the ''null'' events in the study were observed thunderstorms. Many or most of the F1/F2 events were associated with supercells and all of the F0 events were associated with convective storms that may or may not have been electrified. For simplicity, the authors use the term ''tornadic convection'' and ''tornadic thunderstorm'' interchangeably in the text.

* Current affiliation: Cooperative Institute for Mesoscale Meteorological Studies, University of Oklahoma, Norman, Oklahoma.

Corresponding author address: Dr. John P. Monteverdi, Dept. of Geosciences, San Francisco State University, 1600 Holloway Ave., San Francisco, CA 94132.
E-mail: montever@sfsu.edu

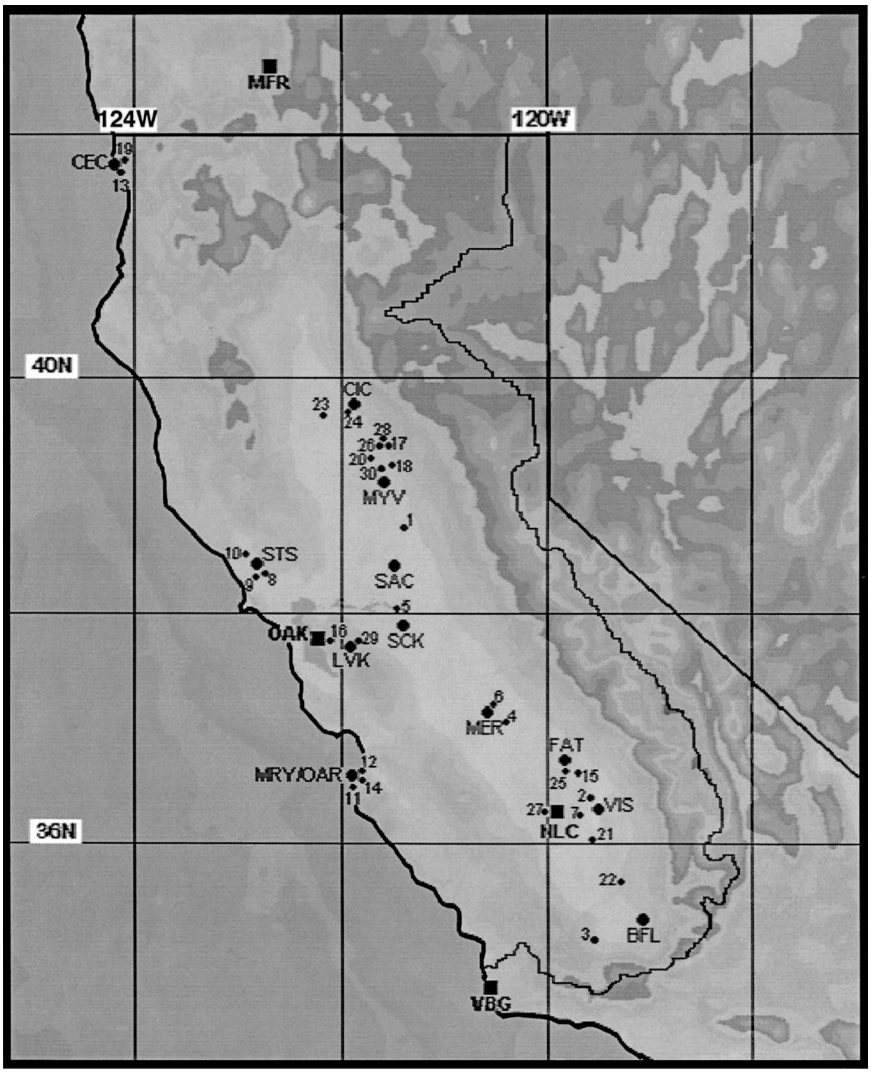

FIG. 1. Locations of verified tornadoes in the period 1990–94, as discussed in the text and listed in Table 1. Locations of surface observation sites (circles) and radiosonde sites (squares) referred to in text also given.

period. Most of the tornado cases and all of the null cases occurred in California's Central Valley (Fig. 1).

The LM dataset was expanded with the null cases to provide a ''control'' on the tornado cases. We originally hoped to provide California forecasters with a way to distinguish the buoyancy and shear environments associated with nontornadic thunderstorms from those associated with tornadic thunderstorms. The basis for this hope stemmed from the few studies in the literature documenting recent supercellular[2] tornado events in this portion of the state. Although our original expectation remains unfulfilled with respect to buoyancy, there is justification for optimism that low-level shear values can be used to distinguish the strongest tornado events.

This study is organized in the following manner. An overview of the typical synoptic-scale pattern associated with tornadic thunderstorms in the Central Valley is presented first. This is followed by a discussion of the buoyancy and shear characteristics associated with both the null and tornadic thunderstorm cases (or bins). The tornado cases are stratified into F0 and F1/F2 groupings or bins based upon shear values. Finally, preliminary forecast thresholds for distinguishing tornadic from nontornadic thunderstorms are suggested on the basis of 0–1- and 0–6-km positive shear values (see section 3 for definition of positive shear). Ongoing research objectives are summarized in the final section.

2. California tornadic storms

Tornadic convection in northern and central California generally develops under the relatively low tropo-

[2] A thunderstorm characterized by a deep and persistent mesocyclone.

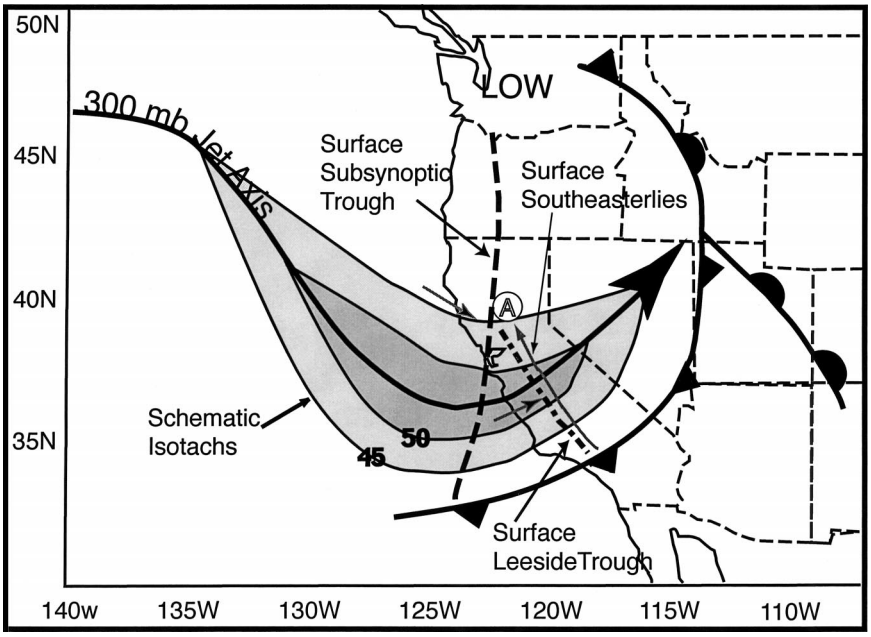

FIG. 2. Schematic chart showing location of major features associated with tornado events in California's Central Valley. Schematic isotachs are labeled in meters per second. Location of subsident flow west of leeside trough and surface southeasterlies in central and eastern Central Valley shown by light gray arrows. The A shows area of major focus for supercell thunderstorm formation as discussed in the text.

pause heights of the winter and spring months in patterns that are conducive to convective storms rooted in the boundary layer. In such buoyant environments, the warm season, inversion-topped surface marine layer is absent and lapse rates are steep in the boundary layer. Soundings correspond to the Miller ''type III'' sounding [for description see Bluestein (1993, p. 453)] and are characterized by steep lapse rates in a relatively shallow layer in the lower troposphere with no significant stable layer (generally referred to as a ''capping inversion'') restraining deep convective motions. Buoyancy, as estimated by common parameters such as convective available potential energy (CAPE), is meager. Because they occur generally in weak buoyancy (i.e., in low CAPE) environments, thunderstorms developing in such an environment are generally low topped, with equilibrium levels typically between 4.5 and 10.6 km (~15 000 and 35 000 ft) (LM).

Climatological analyses (Blier and Batten 1994) show that approximately 80% of the tornadoes that occur statewide are associated with F0 or F1 damage. This figure is somewhat higher than the average fraction of F0 and F1 tornadoes [about 67%; see Kelly et al. (1978)] for the entire United States. In northern and central California, most tornadoes occur in the Sacramento and San Joaquin valleys (together known as the Central Valley) and, to a much lesser extent, the valleys surrounding San Francisco Bay and other coastal sections (Blier and Batten 1994).

Many tornado events occurring in either the Sacramento or San Joaquin valleys are associated with a synoptic pattern (Fig. 2) that acts to create a buoyancy and shear environment favorable for supercell storms. The pattern favoring supercell tornado events in the Central Valley (and, to some extent, in the coastal valleys) initially was described in Monteverdi et al. (1988) and subsequently found to be associated with other cases of tornadic thunderstorms in the state (Braun and Monteverdi 1991; Monteverdi and Quadros 1994; Staudenmaier 1995; Monteverdi and Johnson 1996). Radar documentation of such storms can be found in Carbone (1983), Staudenmaier (1995), Monteverdi and Johnson (1996), Krudzlo (1998), and Monteverdi et al. (2001).

Many northern and central California tornadoes do not form in association with isolated supercell storms. For example, California nonsupercell tornadoes have been documented in zones of intense horizontal shear along fronts (Carbone 1983) and in association with the intersection of bow-echo patterns (Staudenmaier and Cunningham 1996). Tornadoes or funnel clouds also form when isolated nonsupercell storms intercept preexisting vertical vorticity related to topographic interactions or when such storms intercept and tilt solenoidal circulations along outflow and sea-breeze boundaries (Blier and Batten 1994; Monteverdi et al. 2001). Nonsupercellular processes probably account for a relatively large proportion of the tornadoes observed across the state (Blier and Batten 1994).

The low-buoyancy, high-shear environment associated with most of the documented tornadic events in

northern and central California (Braun and Monteverdi 1991; Monteverdi and Quadros 1994; Staudenmaier 1995; Monteverdi and Johnson 1996) is similar to that observed by McCaul and Weisman (1996) for tornadic supercells in hurricane environments. The wind profile features strong low-level shear in the layers with large lapse rates and substantial buoyancy. Most often, the low-level portions of the hodograph are strongly anticyclonically curved. Rotunno and Klemp (1982, 1985), Wicker and Cantrell (1996), and many others have shown that dynamically induced (i.e., attributable to air motion) vertical perturbation pressure gradient forces associated with a veering wind shear vector located generally in the layers of large lapse rate and substantial buoyancy can augment the buoyancy forces by a factor of 2 or more. The combined effects of buoyancy and these dynamically induced accelerations could account for the other manifestations of severe weather (i.e., severe-sized hail, damaging outflow winds, etc.) often observed with California low-topped storms.

An important feature of the synoptic pattern shown in Fig. 2 is that, although the primary frontal system has passed through the northern and central sections of the state, the surface low (usually occluded) is located over the Pacific Northwest. In addition, the main trough axis associated with the mid- and upper-tropospheric disturbance often has not yet passed the coast. The position of these features maintains a synoptic-scale pressure gradient that favors southerly flow over the Central Valley, despite the apparently unfavorable location of the cold front over the southern portion of the state. Topographically induced southeasterly flow is also promoted in the coastal valleys with this pattern.

The trough in the mid- and upper troposphere, schematically shown in Fig. 2, is generally associated with a strong jet stream and favors significant deep-layer (e.g., 0–6 km) shear over the region. Often, a jet streak associated with the trough (shown as schematic isotachs in Fig. 2) is oriented in such a manner that the left exit region, typically associated with upper-tropospheric divergence and large values of subsynoptic upward motion (e.g., Braun and Monteverdi 1991), is located over the area in which the thunderstorms develop.

The west-southwest winds ahead of the trough in the low to midtroposphere are orthogonal to the Coast Range and are associated with leeside troughing at the surface in the western portion of the Central Valley. Topographic channeling acts to create surface southeasterly flow east of the trough axis, which separates the northward-moving air from an air mass that is subsiding along the eastern slopes of the Coast Range.

The southeasterly winds east of the leeside trough in the Central Valley play a central role in the evolution of both the buoyancy and shear environment in the region. The southeasterly winds are associated with warm advection, which act to destabilize the environment north of the synoptic-scale cold front. The southeasterly flow also contributes to a veering wind profile through the midtroposphere. Thus, the most marked low-level (e.g., 0–1 km) shear is also associated with the strongest cross-mountain flow and the strongest deep-layer (e.g., 0–6 km) shear.

Shear profiles in the Sacramento valley are further modified by local topography. Local physiographic features tend to channel surface winds so that they become more backed (e.g., north of the Sutter Buttes near Chico) than the prevailing southeasterly winds associated with this pattern. Finally, the cross-mountain flow over the Sierra Nevada can generate a barrier jet (Parish 1982) about 1500 ft AGL, particularly in the eastern half of the Sacramento valley. The combination of all of these factors can create shear profiles very favorable for rotating storms (Fig. 3).

An additional factor can act to ''focus'' mesoscale destabilization and favorable shear profiles. As the mid- and upper-tropospheric trough progresses southward, cross-mountain flow ceases progressively from north to south. This is evidenced at the surface as a sharp wind shift line (annotated in Fig. 2 as ''Surface Subsynoptic Trough''). The intersection between this feature and the leeside trough is often a focus of thunderstorm development (shown as A in Fig. 2).

Thus, processes associated with this pattern contribute to vigorous lift and enhanced low-level directional and speed shear in favored areas, such as location A shown in Fig. 2. For storms developing in such an environment, the resulting nonhydrostatic pressure perturbation forces generally act within the same layer (lowest 600 mb) in which most of the buoyancy is found, further enhancing the potential for strong updrafts.

3. Methodology

During the 5-yr period 1990–94, 30 tornadoes were documented[3] in northern and central California. The total sample included 16 tornadoes rated F0, 13 F1 tornadoes, and 1 F2 tornado (see Fig. 1 and Table 1). The 30 tornado cases (numbered consecutively in Fig. 1 and Table 1) were grouped into ''tornado events'' on the basis of the proximity sounding/hodograph used in the subsequent analysis. Multiple tornado cases analyzed on the basis of the same proximity sounding/hodograph were counted as single events. This methodology resulted in 25 tornado events (lettered consecutively in Table 1) comprising 30 tornadoes. The statistical analyses in sections 4 and 5 were completed on the basis of these tornado events.

Since most tornado cases in northern and central California occur in the Central Valley, null cases were defined as all days in the period 1990–94 for which thunderstorms were observed either at Sacramento (KSAC)

[3] Only those tornadoes that were tallied in *Storm Data* were included in this study.

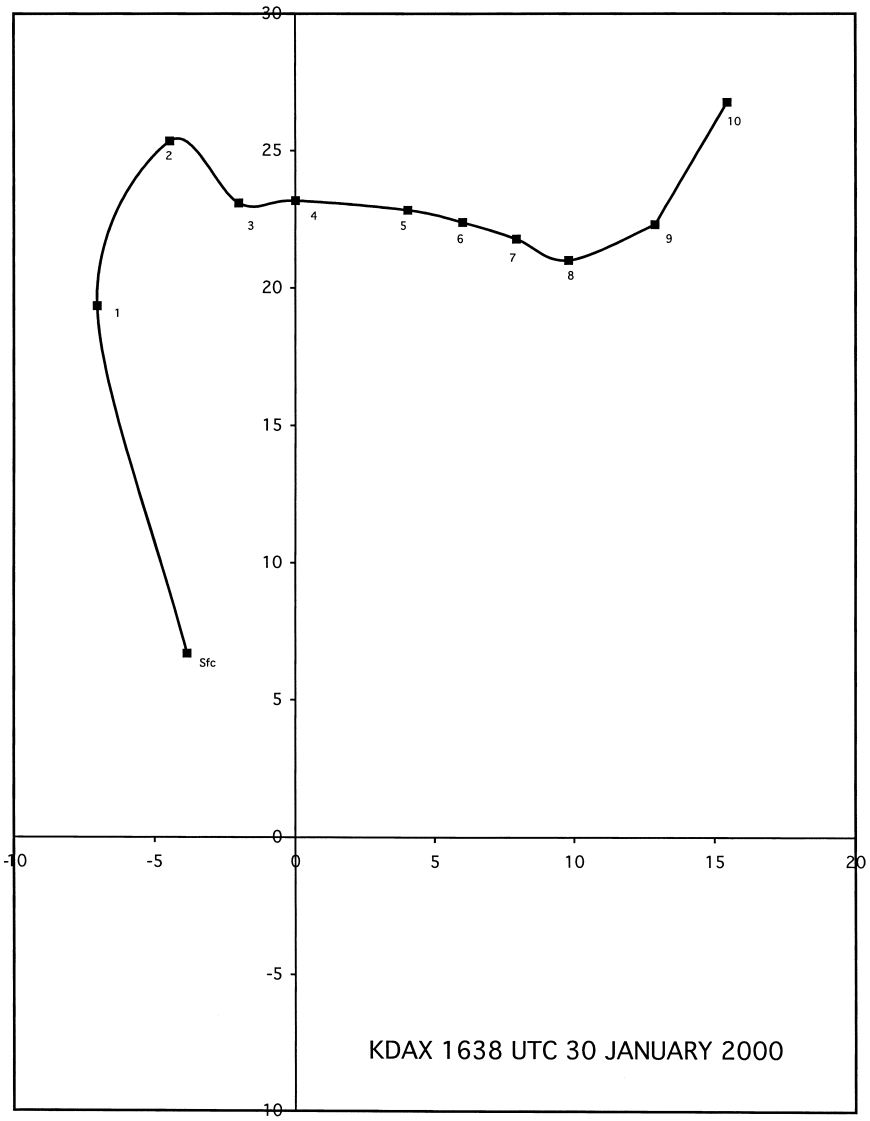

FIG. 3. Hodograph of KDAX WSR-88D vertical azimuth display (VAD) for 0638 UTC 31 Jan 2000, showing influence of low-level jet at approximately 1000 and 2000 ft (300 and 600 m). Hodograph points labeled in 1000s of feet and plotted at 1000-ft (approximately 300 m) intervals; wind speeds in knots.

(as representative of the Sacramento valley) or Fresno (KFAT) (as representative of the San Joaquin valley) but no tornadoes were tallied in *Storm Data*. Both KSAC and KFAT had hourly surface observations during the period. Forty-one null cases were uncovered using this technique (see Table 2) and soundings were available for 39 of them. Interestingly, 23 of 25 tornado events occurred in the cool season (November–April), while 18 of 41 null events took place in the warm season. The fact that only 66 total events occurred in the 5-yr study period in northern and central California is illustrative of the relative rarity of thunderstorm events in general in this portion of California.

Proximity soundings were constructed by modification (described below) of the nearest operational radiosonde for the time closest to the tornado or thunderstorm (for the null cases) occurrence. The authors acknowledge that what makes a sounding ''representative'' of the proximity environment of a thunderstorm remains unresolved. Brooks et al. (1994) summarize the perils associated with trying to define the convective ''environment'' with a sounding. The preconvective ''environment'' is not homogeneous, and once convection gets going, it alters its surroundings significantly. This makes it clear that there are essentially two paths that can legitimately be followed: 1) use the nearest sounding in space and time, subject to some set of criteria about the time–space distance, or 2) interpolate upper-air data to the time and

TABLE 1. Tornado location indicated by map No. (see Fig. 1), damage rating, date and time of tornado and corresponding proximity sounding (as defined in text), location of proximity sounding with azimuth and distance (km) to tornado location, and event identifier (letters group tornadoes by proximity sounding used).

Map No.	Tornado location	Damage rating	Tornado time (UTC)/date	Time (UTC)/date proximity sounding	Proximity sounding location	Azimuth, range (°, km) proximity sounding to tornado location	Event ID
1	Penryn	F0	2330, 23 Apr 1990	2330, 23 Apr 1990	Sacramento (SAC)	015, 45	A
2	Goshen	F1	0015, 01 Mar 1991	0000, 01 Mar 1991	Visalia (VIS)	330, 10	B
3	Taft	F1	0330, 18 Mar 1991	0300, 18 Mar 1991	Bakersfield (BFL)	250, 50	C
4	Chowchilla 6SW	F0	2230, 20 Mar 1991	2200, 20 Mar 1991	Merced (MER)	120, 25	D
5	Lodi 5W	F0	0115, 27 Mar 1991	0100, 27 Mar 1991	Stockton (SCK)	350, 15	E
6	Plainsburg	F0	0200, 27 Mar 1991	0200, 27 Mar 1991	Merced (MER)	035, 10	F
7	Hanford–Corcoran	F0	0515, 12 Oct 1991	0400, 12 Oct 1991	Lemoore (NLC)	100, 35	G
8	Sebastopol 1	F1	2300, 02 Dec 1992	2200, 02 Dec 1992	Santa Rosa (STS)	175, 10	H
9	Sebastopol 2	F1	2300, 02 Dec 1992	2200, 02 Dec 1992	Santa Rosa (STS)	180, 10	
10	Windsor	F1	2300, 02 Dec 1992	2200, 02 Dec 1992	Santa Rosa (STS)	320, 15	
11	Carmel	F1	0100, 07 Dec 1992	0000, 07 Dec 1992	Monterey (MRY)	190, 10	I
12	Monterey	F1	0100, 07 Dec 1992	0000, 07 Dec 1992	Monterey (MRY)	Less than 5 km	
13	Crescent City	F1	1915, 11 Dec 1992	1900, 11 Dec 1992	Crescent City (CEC)	Less than 5 km	J
14	Fort Ord	F0	0045, 12 Dec 1992	0000, 12 Dec 1992	Fort Ord (OAR)	Less than 5 km	K
15	Easton	F0	0050, 12 Dec 1992	0000, 12 Dec 1992	Fresno (FAT)	190, 15	L
16	Oakland	F0	1830, 17 Dec 1992	1800, 17 Dec 1992	Oakland (OAK)	Less than 5 km	M
17	Oroville	F1	2220, 17 Dec 1992	2200, 17 Dec 1992	Marysville (MYV)	360, 55	N
18	Loma Rica	F1	2330, 17 Dec 1992	2200, 17 Dec 1992	Marysville (MYV)	020, 25	
19	Crescent City	F1	0930, 30 Dec 1992	0900, 30 Dec 1992	Crescent City (CEC)	Less than 5 km	O
20	Biggs	F1	2300, 07 Jan 1993	2200, 07 Jan 1993	Marysville (MYV)	340, 30	P
21	Tipton	F0	0115, 20 Feb 1993	0100, 20 Feb 1993	Lemoore (NLC)	130, 60	Q
22	McFarland	F0	2205, 23 Feb 1993	2100, 23 Feb 1993	Bakersfield (BFL)	330, 35	R
23	Willows 3ENE	F1	2340, 17 Apr 1993	0000, 18 Apr 1993	Chico (CIC)	250, 35	S
24	Chico	F0	0020, 18 Apr 1993	0000, 18 Apr 1993	Chico (CIC)	Less than 5 km	
25	South Fresno	F0	2205, 05 Jun 1993	2200, 05 Jun 1993	Fresno (FAT)	180, 5	T
26	Oroville	F2	2228, 10 Feb 1994	2200, 10 Feb 1994	Marysville (MYV)	360, 55	U
27	Lemoore	F0	2245, 05 Mar 1994	2100, 05 Mar 1994	Lemoore (NLC)	Less than 5 km	V
28	Oroville	F0	0330, 11 Mar 1994	0200, 11 Mar 1994	Marysville (MYV)	360, 55	W
29	Livermore	F0	1850, 25 Apr 1994	1800, 25 Apr 1994	Livermore (LVK)	Less than 5 km	X
30	Honcut	F0	0310, 26 Apr 1994	0200, 26 Apr 1994	Marysville (MYV)	345, 15	Y

space location of the event. Both methodologies merely attempt to estimate the environmental conditions that arise from the synoptic-scale environment rather than attempting to re-create the actual buoyancy and shear characteristics for the evervarying microscale environment around the developing storm. We have followed option 1 in this study, as have many others (e.g, Davies-Jones et al. 1990; Brooks et al. 1994).

The Skew-T/Hodograph Analysis and Research Program (SHARP) (Hart and Korotky 1991) was used to construct proximity soundings and hodographs. The ''parent'' soundings were either the 0000 or 1200 UTC Oakland (KOAK), Medford (KMFR), Lemoore Naval Air Station (KNLC), or Vandenberg (KVBG) radiosonde, whichever was closest in space to the tornado or thunderstorm (for the null cases) events. The soundings and hodographs were created by inserting the observed vector storm motion and surface data (T, T_d, vector wind) from the nearest surface reporting station (see Table 1) and for the time immediately preceding that of the tornadic thunderstorm into the observational sounding nearest to the tornado event and at the time closest to the event for the F0 and F1/F2 cases. This criterion ensured that all tornado occurrences were no more than about 180 km (100 n mi) from the observational sounding utilized in the analyses.[4] Null event proximity soundings and hodographs were obtained in a similar manner, except by insertion of the hourly information at either KSAC or KFAT for the hour closest in time to thunderstorm occurrence for the null cases (Table 2).

Buoyancy was calculated on the basis of the CAPE of a surface lifted parcel (SBCAPE) and wind shear parameters were calculated from the proximity hodographs. Surface-based superadiabatic layers that appeared were eliminated by assuming dry-adiabatic conditions from the surface temperature to the intersection with the original sounding.

Two types of shear values were calculated: positive

[4] Most of the tornado events occurred within 3 h of the synoptic sounding times, although several occurred between 4 and 6 h. The authors realize that these latter cases strain the concept of synoptic timescaling. But given the relatively small numbers of tornado events considered in this pilot study, the authors retained these cases. As will be seen below, even this relatively coarse manner in defining ''proximity'' soundings apparently captured the essence of the environmental conditions approximated by the synoptic-scale environment.

TABLE 2. Dates of null events during the period 1990–94, inclusive, at Sacramento Municipal Airport (SAC) and Fresno Air Terminal (FAT), as discussed in text.

SAC Date	FAT Date
12 Jan 1990	13 Jan 1990
16 Jan 1990	18 Feb 1990
28 Feb 1991	4 Mar 1990
1 Mar 1991	21 Sep 1990
10 Mar 1991	23 Sep 1990
20 Apr* 1991	25 Mar 1991
18 Jul 1991	25 Sep 1991
19 Jul 1991	12 Feb 1992
14 Aug 1991	15 Feb 1992
26 Sep 1991	5 Mar 1992
28 Dec 1991	22 Mar 1992
12 Feb 1992	5 May 1992
13 Feb 1992	6 May 1994
14 Feb 1992	30 May 1994
15 Feb 1992	19 Sep* 1994
6 Mar 1992	
13 Jun 1992	
18 Feb 1993	
12 May 1993	
25 May 1993	
4 Jun 1993	
5 Jun 1993	
4 Oct 1993	
15 Dec 1993	
18 May 1994	
4 Oct 1994	

* Sounding information missing.

shear and bulk shear. *Positive*[5] *shear* is defined as the sum of the shear magnitudes for segments of the hodograph in which wind veers or is unidirectional with height (Johns et al. 1990, 1993). Positive shear is greatest for hodographs in which both the wind shear magnitude is great and the wind shear vector veers with height (the hodograph is anticyclonically curved), in the Northern Hemisphere. *Bulk shear* is defined as the vector difference between top and bottom of the specific layers (0–1, 0–2, 0–3, and 0–6 km all AGL) updated with surface observations.

Anticyclonically curved hodographs with sufficient deep-layer shear magnitudes are associated both in modeling results and in field observations with right-propagating supercells that develop the deepest and strongest mesocyclones (Weisman and Klemp 1982). This is because in environments characterized by strongly curved hodographs (in the anticyclonic sense), both linear and nonlinear shear-induced vertical perturbation pressure gradient forces act to promote continuous updraft development on the right flank of the initial storm, thus causing a supercell that moves strongly off the hodograph (Rotunno and Klemp 1982). For a given hodograph length, greater hodograph curvature results in more intense linear dynamic vertical perturbation pressure gradient forces, more significant positive shear, greater deviate (i.e., off the hodograph) storm motion, and stronger mesocyclones.

Although with either straight or curved hodographs, *nonlinear* forcing for dynamic vertical perturbation pressure forces develop. Rotunno and Klemp (1982) and many others have shown that for an anticyclonically curved hodograph, additional *linear*, nonhydrostatic pressure forces enhance updraft development on the storm's right flank. Thus, while ''bulk'' or ''vector difference'' shear for a straight and curved hodograph of a given length may be identical, positive shear generally is larger with curved hodographs.

Dynamic pressure forces play a very important role in situations where storms develop in low-buoyancy/high positive shear environments. The linear pressure forces associated with the strong shear environments characterized by curved hodographs promote much more intense (and rotating) updrafts than might otherwise be expected, given the meager buoyancy alone. McCaul and Weisman (1996) substantiated these effects for hurricane-related storms as did Wicker and Cantrell (1996) for ''minisupercells'' occurring in the Great Plains.

Positive shear was favored in this study because of the relationship of positive shear to the vertical perturbation pressure gradient forces outlined above. We anticipated that with the strongly curved hodographs present in California tornadic patterns, positive shear would provide a meaningful estimate of the situations in which hodographs are most favorable for the development of supercell storms. None of the hodographs for the cases considered in this study were negatively (cyclonically) curved.

Bulk shear was calculated because it is more robust (statistically) than positive shear. Positive shear values can be sensitive to small curvature changes in the hodograph, while bulk shear values are relatively resistant to such variations in the hodograph. In addition, forecasters attempting to assess the vertical wind shear environment can easily calculate bulk shear by simple vector subtraction.

4. Mean buoyancy values

We first attempted to determine if there was a relationship between buoyancy alone and the tendency for thunderstorms to become either tornadic or nontornadic. The impetus for this was simply to test the notion, still widely accepted within the operational forecasting community in California, that the amount of buoyancy is related to the potential for thunderstorms to become tornadic. In addition, we also hoped to determine if there was a tendency for the strongest tornado events (in this case, the F1/F2 bin) to be associated with relatively larger values of SBCAPE.

When SBCAPE values for the cases are grouped into

[5] The term ''positive'' is used to imply that the sense of the shear would be to create streamwise horizontal vorticity that can be converted into *positive* (cyclonic) vertical vorticity by the updraft.

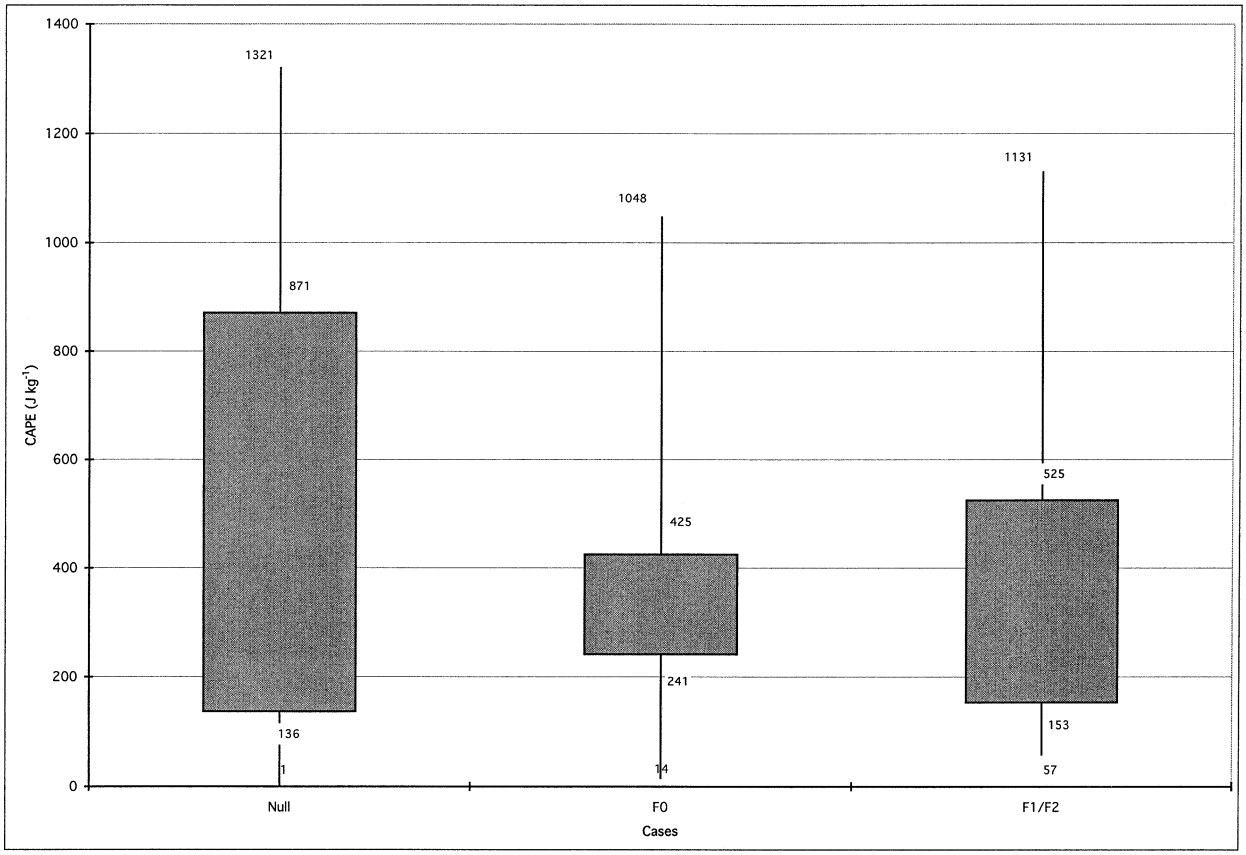

FIG. 4. Maximum, 75th, and 25th percentile and minimum values of SBCAPE observed for the null, F0, and F1/F2 bins.

null, F0, and F1/F2 data groupings (hereafter referred to as bins) (Fig. 4), the median value (near the center of the box in the plot) is less than 500 J kg^{-1} for each of the bins. Since the data were not normally distributed, the authors used the Mann–Whitney test[6] (Johnson 2000, 314–317) to compare the median values for each of the bins. The test failed to show any statistically significant differences in the median values between any pair of the bins. Thus, there appears to be no statistical justification for stratifying the cases on the basis of SBCAPE; there is simply no relationship between buoyancy magnitude *alone* and the potential for thunderstorms to become tornadic. Observe that the greatest mean and maximum buoyancy occurred in the null bin. This result is inconsistent with the notions of those forecasters who persist in believing that threat of tornadoes increases when the SBCAPE increases.

[6] This test is a nonparametric rank-randomization two-sample test that replaces the *t* test when distributions are highly skewed. This test works by ranking all the values for each pair of bins considered from low to high and comparing the mean rank in the two groups. The key result is a significance (*P*) value that answers the following question: if the data bins have the same mean, what is the chance that random sampling would result in means as far apart (or more so) as observed in the test?

5. Positive and bulk shear values

We next examined the relationship of shear values to tornadic thunderstorm potential by considering the mean positive and bulk shear values for each of the bins. Histogram plots of mean shear values for each of the bins (plot for positive shear given in Fig. 5; plot for bulk shear not shown) indicate that shear values for each of the assessed layers increase from null to F0 and from F0 to F1/F2, with the largest relative increases in the 0–1- and 0–6-km layers from F0 to F1/F2 bins.

Box-and-whisker plots of positive shear (Fig. 6) and bulk shear (Fig. 7) values emphasize the striking differences between the shear environments for the F1/F2 cases and those for either the F0 or the null cases. Note that middle 50% of the distributions (i.e., within the plotted box) for the F1/F2 cases for 0–1- and 0–6-km positive shear (Fig. 6) do not overlap most of the data arrays shown for the other two bins, although the differences are not quite so evident for the bulk shear values (Fig. 7).

A Mann–Whitney test was performed on the 0–1- and 0–6-km shear data arrays for the F1/F2 and F0 bins, the F0 and null bins and the F1/F2 and null bins. The most highly statistically significant differences (at the

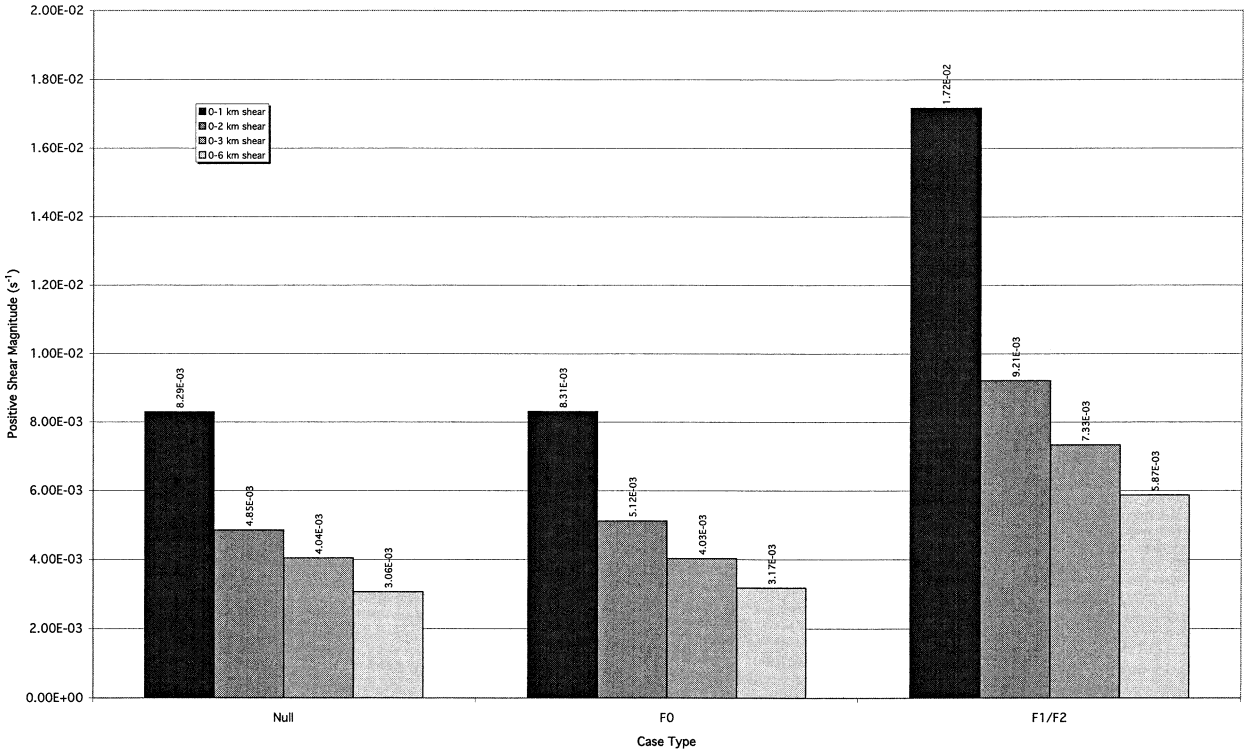

FIG. 5. Mean positive shear values for 0–1-, 0–2-, 0–3-, and 0–6-km layers for the null, F0, and F1/F2 data bins.

1% level)[7] were found between the 0–1- and 0–6-km mean positive shear values for the F1/F2 bins and both those for the F0 and for the null cases. The differences between the 0–1-km mean positive shear values for the F0 and null bins were not found to be statistically significant, while the difference between the 0–6-km mean positive shear for the F0 and null bins was statistically significant at the 5% level.

Although bulk shear values (Fig. 7) for each of the bins show a stratification similar to that of the positive shear values (Fig. 6), it is interesting to note that considerable overlap of the bulk shear data arrays is present. This is consistent with the result of the Mann–Whitney test performed on the bulk shear arrays, which showed that differences between mean bulk shear values for all of the layers considered for the F1/F2 cases and both those for the F0 cases and for the null cases were statistically significant but only at the 5% level.

These results suggest that, at least within our limited dataset, positive shear values are more reliable than bulk shear values at discriminating between thunderstorms that produce F1/F2 tornadoes and those that either produce F0 tornadoes or none at all. Although F1/F2 cases are associated with larger positive shear values for all layers, the most significant differences were evident in the 0–1- and 0–6-km layers. This supported our expectation that a controlling factor in whether or not thunderstorms produce F1 or stronger tornadoes is the strength of the low-level shear in the buoyant inflow layer, given that the deep-layer shear is also favorable for mesocyclogenesis (i.e., formation of supercell storms).

This result is consistent with that observed for other tornado datasets (see, e.g., Johns and Doswell 1992) in which strong-to-violent supercell tornado events in lower-buoyancy environments in the midsection of the United States are associated with stronger low-level shear values (e.g., 0–1- and 0–2-km positive shear) than those observed with higher-buoyancy cases. The inference to be made is that there are various combinations of buoyancy and shear that permit supercell tornadogenesis, regardless of rated tornado intensity. In low-buoyancy environments in which the deeper-layer shear is sufficient for supercells, vertical perturbation pressure gradient forces related to low-level shear (as outlined in section 3) are significant in augmenting the updraft.

It is also interesting to note that the deep-layer bulk shear (i.e., 0–6-km shear) values observed for the F1/F2 bins are similar to those used in modeling studies of supercell thunderstorms. For example, Weisman and Klemp (1982) point out that modeled thunderstorms

[7] Since six independent null hypotheses regarding positive shear were tested by the authors, there was a 26% chance [from the formula $100(1.00 - 0.95^N)$] of obtaining at least one statistically significant result at the 5% level by chance alone. Thus we set a stricter threshold significance value for each individual comparison [from the formula $(1.00 - 0.95^N)$] ensuring that positive shear differences were statistically significant at least at the 5% level.

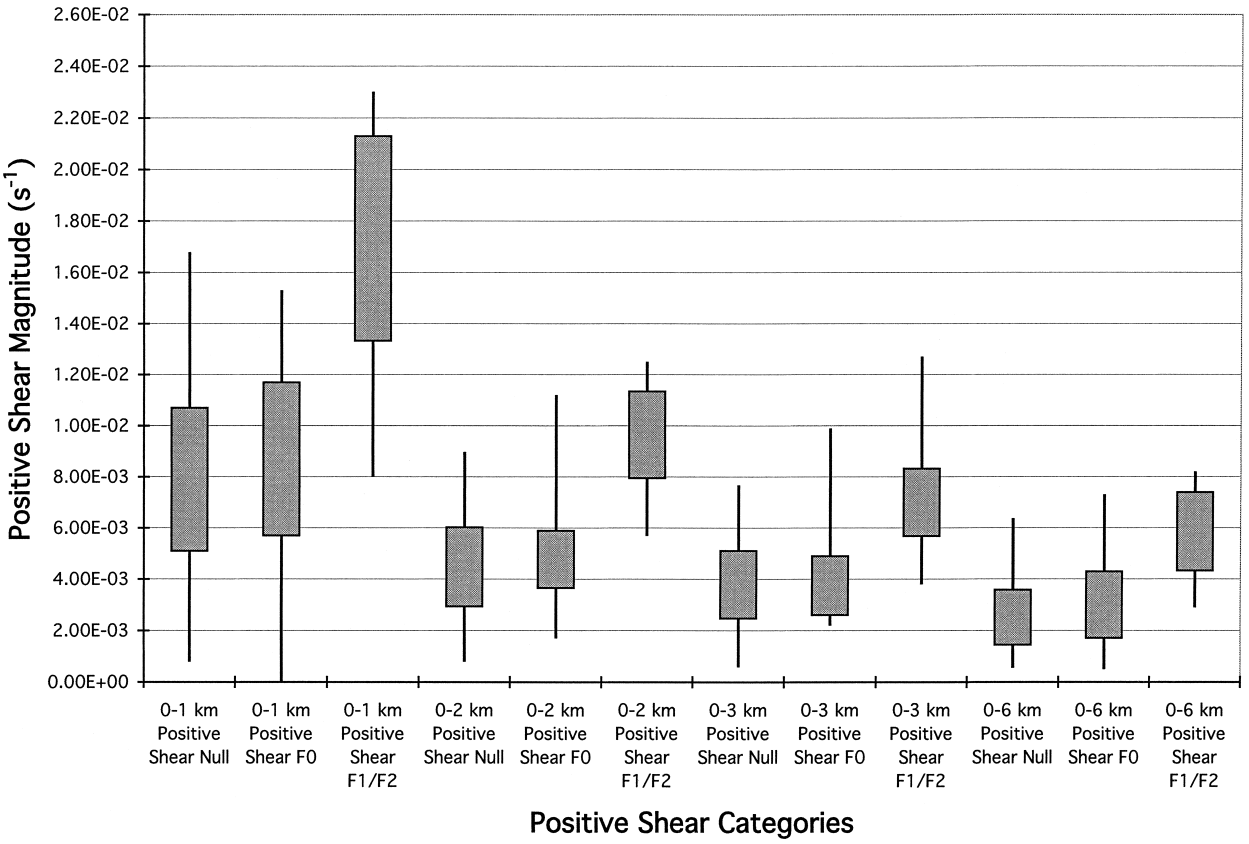

FIG. 6. Maximum, 75th, and 25th percentile and minimum values of positive shear observed for the null, F0, and F1/F2 bins for various layers.

growing in an environment of moderate shear (i.e., 3×10^{-3} s^{-1} to 5×10^{-3} s^{-1}) show an increasing tendency for organization and supercell characteristics, whereas those growing in an environment of strong shear (i.e., $>5 \times 10^{-3}$ s^{-1}) develop the most persistent and strong mesocyclones. In addition, the large 0–1- and 0–2-km positive shear magnitudes for the F1/F2 bin are consistent with those found in observational studies of tornadoes associated with rotating thunderstorms in environments with favorable deep-layer shear for supercells (Johns et al. 1990; Johns and Doswell 1992). Hence, the shear values associated with the F1/F2 events in this study are consistent with those observed with supercell thunderstorms observed elsewhere in the country.

For the tornado cases, low-level shear increases as the deep-layer shear increases; a result consistent with the model presented in section 2. When the 0–6-km shear is the greatest, mid- and upper-tropospheric winds are strongest against the mountains; this promotes a low-level jet, strong southeasterly flow in the eastern sections of the Central Valley, and high values of low-level shear.

We recognize that the statistical analyses and the inferences drawn from them are grounded upon a rather limited dataset. Thus, we consider these results to be preliminary and realize that only an analysis of the complete dataset for California tornadoes (~140 tornadoes between 1951 and 2000) will determine whether the results from this pilot study are representative.

6. Proposed shear thresholds for tornado forecasting

The results summarized in the previous section suggested to the authors that California forecasters already anticipating convective storms in the northern and central portions of the state on the days on which the 39 ''null'' and 25 ''tornado'' events occurred could have used positive shear thresholds as a means of assessing the risk that the developing storms would have become tornadic. We hasten to point out that the following discussion is based upon analyses of a small sample of cases (despite the statistical significance of the results, discussed in the previous section) and is only suggestive of possible forecast thresholds. In this section, we examine what would result if forecasters during the period 1990–94 had applied the shear thresholds proposed in this study in making an assessment of the risk for tornadic convection. The discussion that follows is predicated on the notion that forecasters already would have anticipated convective storms on the days in question and should not be interpreted as a methodology of fore-

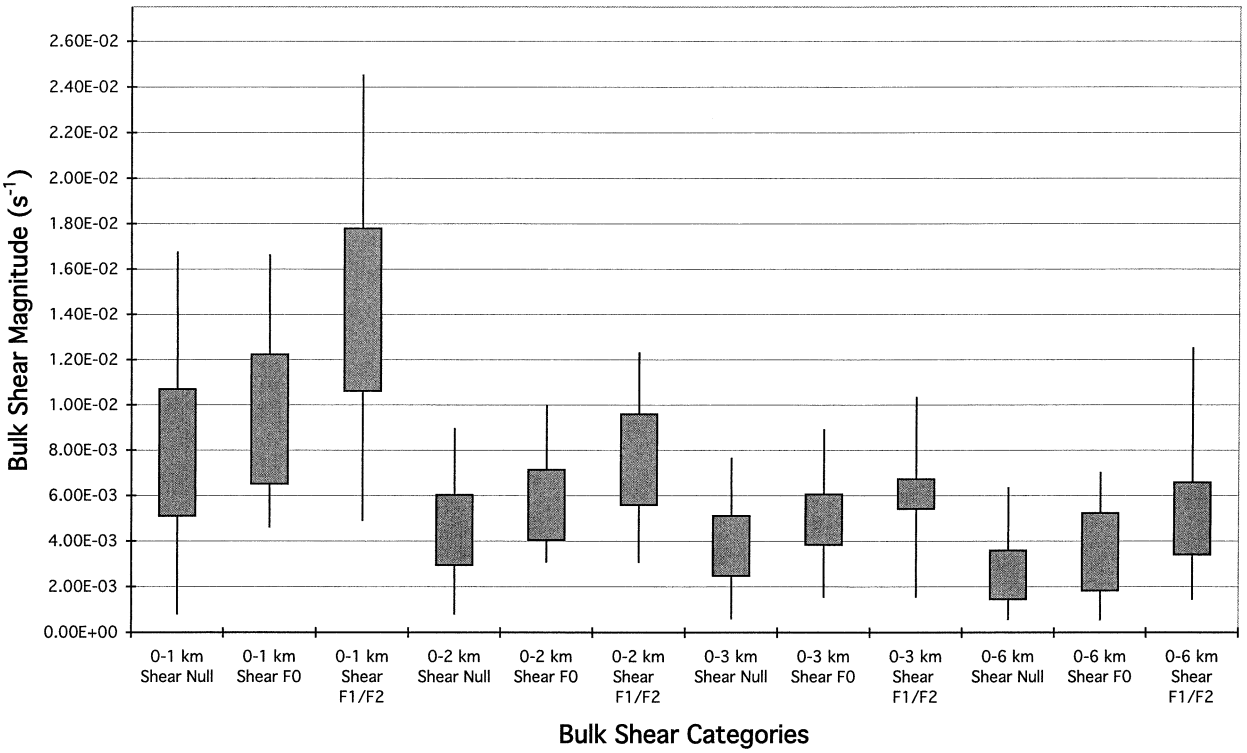

FIG. 7. Maximum, 75th and 25th percentile and minimum values of bulk shear observed for the null, F0, and F1/F2 bins for various layers.

casting thunderstorms in general. The results summarized below should be considered as preliminary until a larger dataset can be tested.

The plots in Figs. 6 and 7 show that although shear values alone would not have helped forecasters already anticipating thunderstorms in distinguishing the risk for the weak tornado events versus the nontornadic thunderstorm events, a *combination* of 0–1- and 0–6-km positive and bulk shear would have discriminated between the stronger tornado events from the F0 and null events. Consequently, we defined thresholds for both the 0–1- and 0–6-km shear values beyond which a forecaster could have anticipated a large majority (at least 75%) of the F1/F2 tornadoes. Threshold shear values that met that criterion then were defined in the following manner: (a) to capture only tornado events (with no null events), (b) to capture all of the F1/F2 tornadoes, and (c) to capture roughly half of all tornado events, as shown in Table 3.

To explore the forecast capability of the shear values, we used shear value pairs (0–1- and 0–6 km) as ''forecast'' thresholds and calculated probability of detection (POD) and false alarm ratio (FAR) for any tornado and for F1/F2 tornadoes for each of the threshold shear pairs (Fig. 8). Note that only the results for the positive shear thresholds are presented here, because the large overlap of bulk shear values for each of the bins evident in Fig. 7 had the result of producing unacceptably large values of FAR (i.e., >0.50) for the threshold pairs based upon bulk shear.

The lowest threshold shear values to ''capture'' only tornado events that occurred in 1990–94 were used in a ''forecast retrospective'' (hindcast) for the potential of tornadic thunderstorms regardless of F rating. Thus, if forecasters during that period had used a threshold value of $7.4 \times 10^{-3}\ s^{-1}$ 0–1-km positive shear in combination with a value of $5.0 \times 10^{-3}\ s^{-1}$ 0–6-km positive shear (solid box in Fig. 8) to forecast the potential for tornadic thunderstorms, they would have correctly not included any null cases. This is reflected in an FAR of

TABLE 3. POD and FAR for positive shear thresholds corresponding to (a) solid box, (b) dashed box, and (c) dotted box in Fig. 8. Shear is in ($\times 10^{-3}\ s^{-1}$), and POD in (%)/FAR is a ratio.

Threshold capture at least 75% of F1/F2 events and	0–1-km positive shear	0–6-km positive shear	POD/FAR all tornadoes	POD/FAR F1/F2 tornadoes
(a) No nulls	7.4	5.0	36/0.00	76/0.22
(b) All F1/F2s	7.4	2.5	56/0.30	100/0.50
(c) POD all tornado 45%	12.5	3.0	44/0.08	80/0.33

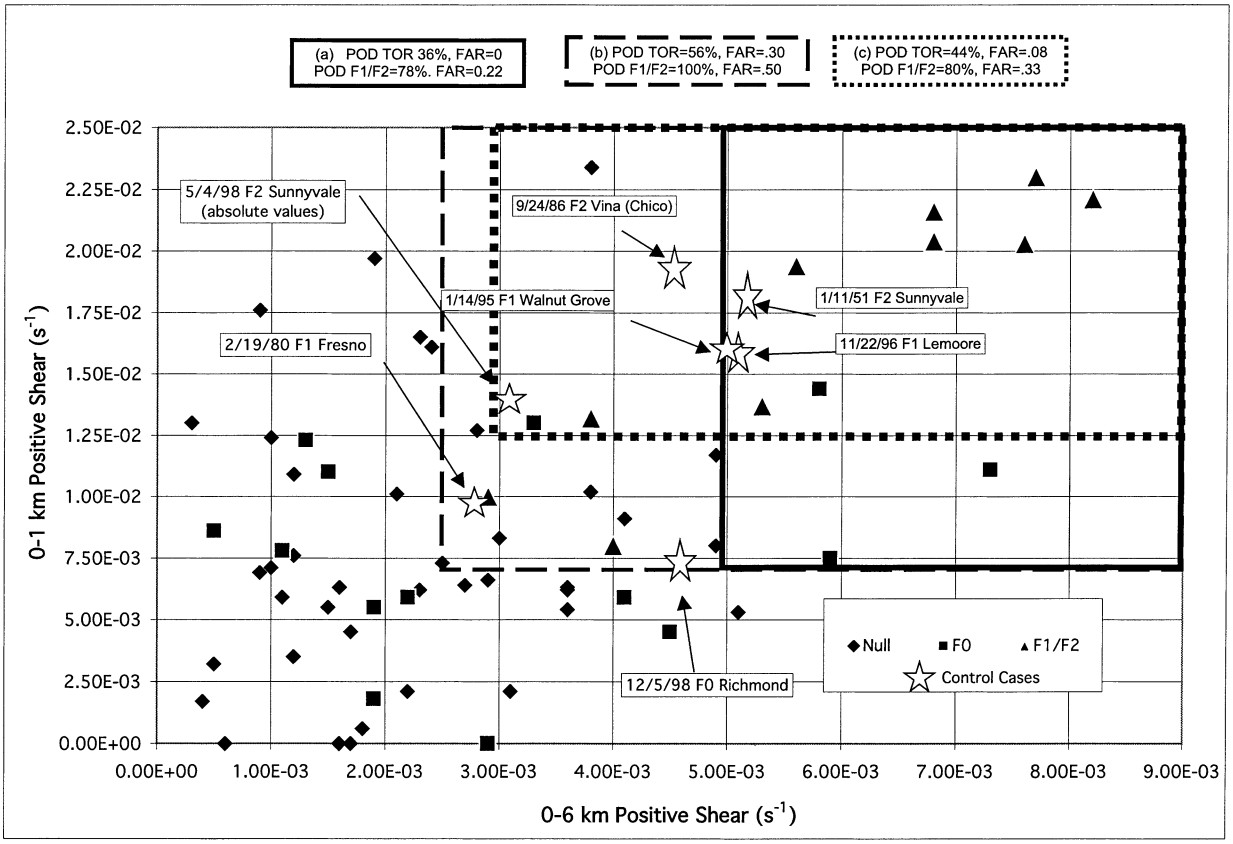

FIG. 8. Positive shear values for the 64 cases included in the study (diamonds = null; filled squares = F0, and triangles = F1/F2). Boxes labeled (a), (b), and (c) correspond to thresholds as summarized in Table 3. Shear values for notable California tornado cases not occurring in 1990–94 but used as controls (Table 4) are indicated as open stars. (Note: the 4 May 1998 Sunnyvale tornado occurred in a cyclonic or negative shear environment and values shown are absolute. All other storms occurred in environments that exhibited anticyclonically curved hodographs and, thus, a positive shear.)

0.0. However, there were many tornadoes that occurred with positive shear magnitudes smaller than the threshold values, and this is reflected in a POD of only 36%. Interestingly, a forecaster using the same shear threshold values to forecast the potential for F1/F2 tornadoes would have had a POD of 78%, but an FAR of 0.22, because several of the events in this domain produced F0 tornado events.

A threshold pair of 0–1- and 0–6-km positive shear values was set to include all F1/F2 events during the period (dashed box in Fig. 8). The POD for F1/F2 using this set of threshold values was a perfect 100%, yet with a significant FAR, because both F0 tornadoes and nontornadic thunderstorms also occurred with shear values in this domain. Note that other shear combinations could have been used to achieve a POD for F1/F2 tornadoes of 100%, but these would have had an unacceptably large FAR (i.e., >0.50).

Finally, a threshold pair of 0–1- and 0–6-km positive shear values was set to include roughly half of the tornado events (dotted box in Fig. 8). Only 8% of the events that occurred with shear magnitudes larger than these limits were nontornadic, leading to a very low FAR. However, forecasters would have missed many F0 events that occurred with lower values of shear. Interestingly, a forecaster using these same limits to anticipate F1/F2 tornadoes during the period, would have anticipated 80% of those, with an FAR of only 0.33. Thus, forecasters using these thresholds would have had reasonable success in forecasting the potential for tornadic thunderstorms during the period and also would have correctly forecast most of the stronger, possibly supercellular events, with a reasonably low FAR.

We also calculated positive shear values for several noteworthy and damaging tornadoes in California, all of which occurred outside of the 1990–94 period considered in this study (Table 4). Radar data were available and examined for all but one of these test cases to determine the nature of the parent thunderstorm. Of the six cases examined for which radar data were available, four were associated with isolated supercells and two with bowed-segment lines of storms (nonsupercellular). The final case was associated with shear values consistent with supercell storms. Six of the cases were F1 or greater.

The shear values for each of the cases is shown in

Table 4. Cases used to test threshold positive shear ($\times 10^{-3}$ s^{-1}). (Note: Sunnyvale tornado associated with negative shear.)

Date	Location	Radar signature	F rating	0–1-km positive shear	0–6-km positive shear
11 Jan 1951	Sunnyvale	NA	F2	18.2	5.2
19 Feb 1980	Fresno	Line	F1	9.80	2.80
24 Sep 1986	Chico (Vina)	Supercell	F2	19.00	4.50
14 Jan 1995	Walnut Grove	Supercell	F1	16.00	5.00
22 Nov 1996	Lemoore	Supercell	F1	15.50	5.20
4 May 1998	Sunnyvale	Supercell	F2	(14.70)	(3.10)
5 Dec 1998	Richmond	Line	F0	7.50	6.00

Table 4, and plotted in Fig. 8. It is interesting to note that all but one of the F1/F2 ''control'' cases would have been anticipated using the second set (b) of threshold values as listed in Table 3. All of the control cases would have been anticipated using the third set (c) of threshold values.

The Sunnyvale case of 4 May 1998 was unusual because the parent thunderstorm was a left-moving anticyclonic supercell (Monteverdi et al. 2001) that developed in a negative (cyclonic) shear environment. Since the absolute value of the shear values for that case fell within the ranges of the positive shear thresholds defined above, this case was included in Table 3.

7. Conclusions

This study of 25 tornadic and 39 nontornadic thunderstorm events in California shows that buoyancy alone could not be used to distinguish between tornadic and nontornadic events. Statistically significant differences in values of 0–1- and 0–6-km shear for the F1/F2 cases compared to the other bins suggest thresholds that could be used in assessing the risk for convection associated with F1/F2 tornadoes in California. This study also shows that positive shear outperforms bulk shear as a forecast parameter, at least in detecting the F1 and stronger events. This is consistent with observational and modeling results that show the association of anticyclonically curved hodographs with stronger tornado events in other parts of the United States. A forecaster in California using the shear thresholds developed in this study would have had considerable success in forecasting the potential for thunderstorms producing the stronger tornadoes (F1/F2), at least for the storms represented in the dataset.

This analysis shows that there is a statistically significant difference between the shear values for F0 storms versus that for F1/F2 storms. Our data do not allow us to determine that (a) the tornadic storms that produced F1/F2 tornadoes were mostly (or entirely) supercells, or (b) the tornadic storms that produced F0 tornadoes were mostly (or entirely) nonsupercells. However, the difference in shear values we have found for the two bins is sufficient to indicate that storms developing in the environment associated with F1/F2 tornadoes are much more likely to have been supercells than those developing in the environments of the F0 events. In fact, we suggest that the most plausible explanation for the occurrence of the stronger F1/F2 events is that the parent thunderstorms were supercells, whereas the F0 storms were nonsupercells, but we recognize that only careful study of the Doppler radar signatures of these storms can validate this assertion. The Weather Surveillance Radar-1988 Doppler (WSR-88D) sites at Monterey (KMUX,) Davis (KDAX), and Hanford (KHNX) were not operational until 1995. Given the relative infrequency of thunderstorms in northern and central California, it will be some years before a comparable dataset with accompanying radar data archives can be assembled for that area.

The possible unreported occurrence of tornadoes among our ''null'' cases cannot be dismissed, owing to the nonvanishing probability of unobserved events. However, the shear values for our null cases are not significantly different from those for the F0 tornadoes. Therefore, any unreported tornadoes are most likely to have been brief and weak. Since nonsupercell tornadoes are largely unrelated to significant deep-layer and/or low-level shear, it is not possible to distinguish F0 tornado days from null days, but the data do support distinguishing between days with F1/F2 events from all others (F0s and nulls) with some accuracy.

We recognize the dangers of inferring too much from the limited data sample considered here. Because of this, the study is being expanded to include all tornadic cases from 1950 to 1989 and from 1995 to the present time. Even so, the success of the thresholds in hindcasting the potential for tornadic convection in general, and for the stronger F1/F2 (possibly supercellular) events in particular, suggests that California forecasters can use shear thresholds to develop a heightened sense of awareness on days when the environment supports an enhanced threat of strong tornadoes in northern and central California.

Acknowledgments. This research was partially funded by the Department of Geosciences, San Francisco State University, and the National Severe Storms Laboratory. Lipari and Monteverdi was partially composed of work in progress by the third author as part of his M.S. thesis in applied geosciences at San Francisco State University. The authors gratefully acknowledge the diligence

of three anonymous reviewers and Josh Korotky in guiding them in the revisions of this manuscript.

REFERENCES

Blier, W., and K. A. Batten, 1994: On the incidence of tornadoes in California. *Wea. Forecasting,* **9,** 301–315.

Bluestein, H. B., 1993: *Synoptic-Dynamic Meteorology in Midlatitudes.* Vol. II, *Observations and Theory of Weather Systems,* Oxford University Press, 594 pp.

Braun, S. A., and J. P. Monteverdi, 1991: An analysis of a mesocyclone-induced tornado occurrence in northern California. *Wea. Forecasting,* **6,** 13–31.

Brooks, H. E., C. A. Doswell III, and J. Cooper, 1994: On the environments of tornadic and nontornadic mesocyclones. *Wea. Forecasting,* **9,** 606–618.

Carbone, R. E., 1983: A severe frontal rainband. Part II: Tornado parent vortex circulation. *J. Atmos. Sci.,* **40,** 2639–2654.

Davies-Jones, R., D. Burgess, and M. Foster, 1990: Test of helicity as a tornado forecast parameter. Preprints, *16th Conf. on Severe Local Storms,* Kananaskis Park, AB, Canada, Amer. Meteor. Soc., 588–592.

Hanstrum, B. N., G. A. Mills, and A. Watson, 1998: Australian cool season tornadoes, Part 1. Synoptic climatology. Preprints, *19th Conf. on Severe Local Storms,* Minneapolis, MN, Amer. Meteor. Soc., 97–100.

Hart, J. A., and J. Korotky, 1991: The SHARP workstation—A skew-T/hodograph analysis and research program. NOAA/NWS NWSFO, 37 pp.

Johns, R. H., and C. A. Doswell III, 1992: Severe local storms forecasting. *Wea. Forecasting,* **7,** 588–612.

——, J. M. Davies, and P. W. Leftwich, 1990: An examination of the relationship of 0-2km AGL ''positive'' shear to potential buoyant energy in strong and violent tornado situations. Preprints, *16th Conf. on Severe Local Storms,* Kananaskis Park, AB, Canada, Amer. Meteor. Soc., 593–598.

——, J. M. Davies, and P. W. Leftwich, 1993: Some wind and instability parameters associated with strong and violent tornadoes: 2. Variations in the combinations of wind and instability parameters. *The Tornado: Its Structure, Dynamics, Prediction and Hazards. Geophys. Monogr.,* No. 79, Amer. Geophys. Union, 583–590.

Johnson, R. A., 2000: *Probability and Statistics for Engineers.* Prentice Hall, 622 pp.

Kelly, D. R., J. T. Schaefer, R. P. McNulty, C. A. Doswell III, and R. F. Abbey Jr., 1978: An augmented tornado climatology. *Mon. Wea. Rev.,* **106,** 1172–1183.

Krudzlo, R., 1998: The Lemoore Naval Air Station classic supercell tornado of 22 November 1996. Western Region NWS Tech. Attachment 98-07, 8 pp.

Lipari, G. S., and J. P. Monteverdi, 2000: Convective and shear parameters associated with northern and central California tornadoes during the period 1990–94. Preprints, *20th Conf. on Severe Local Storms,* Orlando, FL, Amer. Meteor. Soc., 518–521.

McCaul, E. W., Jr., and M. L. Weisman, 1996: Simulations of shallow supercell storms in landfalling hurricane environments. *Mon. Wea. Rev.,* **124,** 408–429.

Monteverdi, J. P., and J. Quadros, 1994: Convective and rotational parameters associated with three tornado episodes in northern and central California. *Wea. Forecasting,* **9,** 285–300.

——, and S. Johnson, 1996: A supercell with hook echo in the San Joaquin valley of California. *Wea. Forecasting,* **11,** 246–261.

——, S. A. Braun, and T. C. Trimble, 1988: Funnel clouds in the San Joaquin valley, California. *Mon. Wea. Rev.,* **116,** 782–789.

——, W. Blier, G. Stumpf, W. Pi, and K. Anderson, 2001: First WSR-88D documentation of an anticyclonic supercell with anticyclonic tornadoes: The Sunnyvale/Los Altos, California tornadoes of 4 May 1998. *Mon. Wea. Rev.,* **129,** 2805–2814.

Parish, T. R., 1982: Barrier winds along the Sierra Nevada mountains. *J. Appl. Meteor.,* **21,** 925–930.

Rotunno, R., and J. B. Klemp, 1982: The influence of shear-induced pressure gradient on thunderstorm motion. *Mon. Wea. Rev.,* **110,** 136–151.

——, and J. B. Klemp, 1985: On the rotation and propagation of simulated supercell thunderstorms. *J. Atmos. Sci.,* **42,** 271–292.

Staudenmaier, M. J., 1995: The February 10 1994 Oroville tornado—A case study. NOAA Tech. Memo. NWS WR-229, 37 pp. [Available from National Weather Service Western Region, P.O. Box 11188, Salt Lake City, UT 84147.]

——, and S. Cunningham, 1996: An examination of a dynamic cold season bow echo in California. NWS Western Region Tech. Attachment 96-10, 5 pp. [Available from National Weather Service Western Region, P.O. Box 11188, Salt Lake City, UT 84147.]

Weisman, M. L., and J. B. Klemp, 1982: The dependence of numerically-simulated convective storms on vertical wind shear and buoyancy. *Mon. Wea. Rev.,* **110,** 504–520.

Wicker, L. J., and L. Cantrell, 1996: The role of vertical buoyancy distributions in miniature supercells. Preprints, *18th Conf. on Severe Local Storms,* San Francisco, CA, Amer. Meteor. Soc., 225–229.